Human Molecular Genetics, 2004, Vol. 13, No. 16 ***1703–1714***
doi:10.1093/hmg/ddh191
Advance Access published on June 22, 2004

Connexin30 mutations responsible for hidrotic ectodermal dysplasia cause abnormal hemichannel activity

Guilherme Munhoz Essenfelder[1,2], Roberto Bruzzone[3,4], Jérôme Lamartine[1,2], Anne Charollais[5], Claudine Blanchet-Bardon[6], Michael T. Barbe[4], Paolo Meda[5] and Gilles Waksman[1,2,*]

[1]Service de Génomique Fonctionnelle, CEA-Evry, 91057 Evry, France, [2]EA2541, Université d'Evry Val d'Essonne, 91025 Evry, France, [3]Department of Neuroscience, Institut Pasteur, 75015 Paris, France, [4]Department of Clinical Neurobiology, IZN, University of Heidelberg, 69120 Heidelberg, Germany, [5]Department of Cell Physiology and Metabolism, University of Geneva, CMU, 1211 Genève 4, Switzerland and [6]Department of Dermatology, CHU Saint Louis, 75010 Paris, France

Received March 16, 2004; Revised May 18, 2004; Accepted June 11, 2004

Clouston syndrome or hidrotic ectodermal dysplasia (HED) is a rare dominant genodermatosis characterized by palmoplantar hyperkeratosis, generalized alopecia and nail defects. The disease is caused by mutations in the human *GJB6* gene which encodes the gap junction protein connexin30 (Cx30). To gain insight into the molecular mechanisms underlying HED, we have analyzed the consequences of two of these mutations (G11R Cx30 and A88V Cx30) on the functional properties of the connexons they form. Here, we show that the distribution of Cx30 is similar in affected palmoplantar skin and in normal epidermis. We further demonstrate that the presence of the wild-type protein (wt Cx30) improves the trafficking of mutated Cx30 to the plasma membrane where both G11R and A88V Cx30 co-localize with wt Cx30 and form functional intercellular channels. The electrophysiological properties of channels made of G11R and A88V Cx30 differ slightly from those of wt Cx30 but allow for dye transfer between transfected HeLa cells. Finally, we document a gain of function of G11R and A88V Cx30, which form functional hemichannels at the cell surface and, when expressed in HeLa cells, generate a leakage of ATP into the extracellular medium. Such increased ATP levels might act as a paracrine messenger that, by altering the epidermal factors which control the proliferation and differentiation of keratinocytes, may play an important role in the pathophysiological processes leading to the HED phenotype.

INTRODUCTION

Clouston syndrome, also referred to as hidrotic ectodermal dysplasia (HED) (MIM 129500), is a rare genetic disorder characterized by three major clinical signs: generalized alopecia, nail dystrophy and palmoplantar hyperkeratosis (1,2). Patients present normal sweating and their cutaneous signs may be accompanied by other symptoms such as mental retardation (3). The syndrome is transmitted in a dominant, autosomal manner and mainly affects the French-Canadian populations (4). A positional cloning study showed that affected individuals from one large French family presented a point mutation (31G > A) in the coding region of the *GJB6* gene, which codes for the gap junction protein connexin30 (Cx30) (5). This mutation leads to the substitution of one amino acid on the N-terminal tail of the protein (mutation G11R). The same study showed that this mutation was present in patients of most families affected by Clouston syndrome, whereas other affected families presented another point mutation (263C > T) leading to an amino acid substitution (A88V) in the second transmembrane domain of Cx30. More recently, a third mutation (110T > A) leading to the amino acid substitution (V37E) has been described in one patient (6).

Connexins (Cx) are a family of proteins that play an important role in cell-to-cell communication, as they constitute the

*To whom correspondence should be addressed at: Service de Génomique Fonctionnelle, 2 Rue Gaston Cremieux, CEA-Evry, 91057 Evry, France. Tel: +33 160873483; Fax: +33 160873498; Email: gilles.waksman@cea.fr

protein subunits of gap junctions. Connexins form hexameres called connexons, which interact with connexons from adjacent cells to form a complete intercellular gap junction channel that provides a pathway for both ionic and metabolic coupling between the participating cells. More than 20 different connexins have been described in mammals so far, each with specific tissue distribution, electrophysiological characteristics and regulatory properties. Still, all connexins share a similar structure comprising four transmembrane domains, and differ mainly by the size and nature of their C-terminal, intracellular tail (7,8). Mutations in some connexins are responsible for genetic diseases, and different mutations of the same connexin can generate a variety of phenotypes (9). For example, Cx26 or Cx31 are responsible for epidermal disorders and/or hereditary hearing impairment [viz. keratitis-ichthyosis-deafness syndrome, Vohwinkel syndrome and non-syndromic hearing impairment for Cx26; erythrokeratodermia variabilis (EKV) and nonsyndromic hearing impairment for Cx31]. Such is also the case for Cx30. Indeed, another point mutation of Cx30 (T5M) is responsible for a recessive form of profound sensorineural deafness (10).

Even though the number of connexin mutations known to be responsible for genetic diseases continues to increase, the molecular mechanisms underlying most connexin-related genodermatosis remain unclear. In an attempt to understand how the G11R and A88V mutations of the human Cx30 generate a skin phenotype, skin of HED patients was immunostained to determine the localization of the wild-type and mutated forms of Cx30 within the epidermis. We also studied the functional properties of the skin-related Cx30 mutations using two different expression systems, to assess how the mutated proteins compare and interact with the wild-type Cx30 (wt Cx30). Our data show that both the G11R and A88V variants retain the ability to form intercellular channels, but also make functional hemichannels that may lead to the abnormal release of paracrine signals. These findings provide novel insights on a possible pathophysiological mechanism whereby Cx30 mutations cause HED.

RESULTS

Cx30 is similarly distributed in normal and HED epidermis

The affected epidermis of Clouston patients (Fig. 1C) showed a marked thickening of the stratum corneum (hyperkeratosis), and the number of living keratinocytes seems slightly increased (mild acanthosis), when compared with normal palmoplantar human epidermis (Fig. 1A). The thicker stratum corneum was compact and did not feature cell nuclei (orthokeratosis), indicating proper terminal differentiation of the affected keratinocytes. In both normal, as previously described (11), and HED palmoplantar skin, Cx30 staining was restricted to keratinocytes of the upper layers of the stratum spinosum and to those of the stratum granulosum (Fig. 1B and D), as well as in sweat gland ducts (data not shown). No detectable intracellular accumulation of Cx30 was observed in the cytoplasm of HED keratinocytes, suggesting that mutant proteins were either rapidly degraded or properly transferred to the membrane, similarly to the wt Cx30.

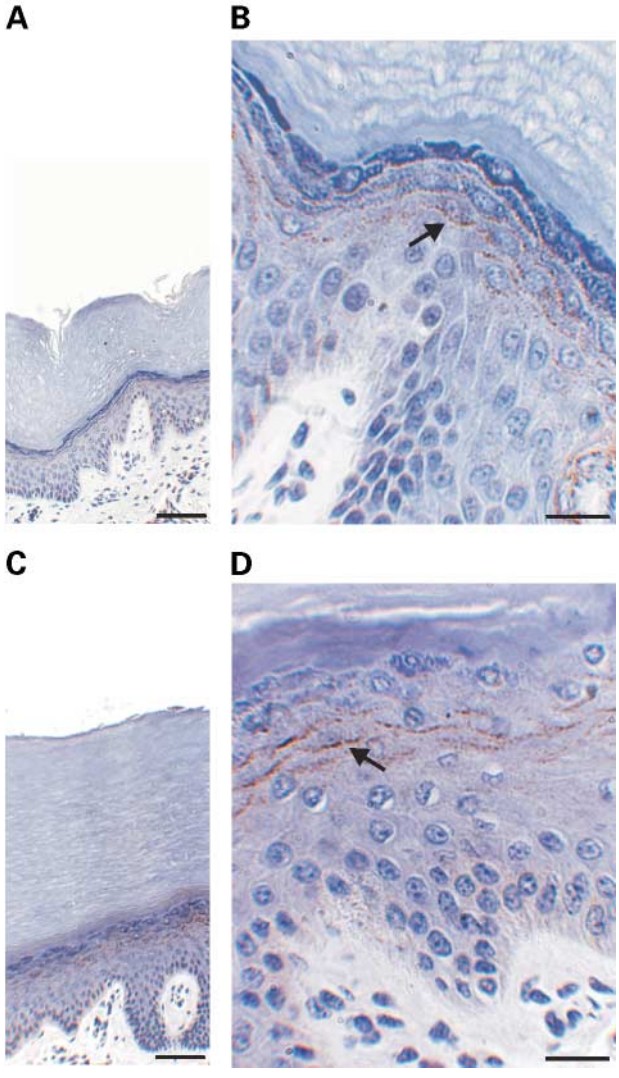

Figure 1. Cx30 shows a similar localization in normal and HED palmoplantar epidermis. (**A**) Immunolabelling of palm epidermis of a control individual (higher magnification in (**B**) shows that wt Cx30 was distributed in the keratinocytes of the upper spinous layers (arrow) and in those of the stratum granulosum. (**C**) Affected palm epidermis of a HED patient, who was heterozygous for the G11R mutation, shows a thickening of the stratum corneum and a mild acanthosis. (**D**) A higher magnification of the affected epidermis shows the normal localization of both wt and mutated forms of Cx30 in the stratum granulosum and stratum spinosum (arrow). Sections were counterstained with haematoxylin. Scale bar 100 μm in A and C, and 20 μm in B and D.

The same membrane sites contain both mutant and wt Cx30

The connexin-deficient HeLa cell line was transiently transfected with plasmids driving the expression of different forms of Cx30. The presence of a V5 tag on the G11R and A88V constructs allowed us to distinguish between the mutated and the wild-type forms of the protein. Wt Cx30 was not recognized by the anti-V5 antibody due to the presence of a stop codon preventing the translation of the tag, but was recognized by the anti-Cx30 antibody and was detected as green fluorescence, thanks to a FITC-labelled anti-rabbit antibody. On the other hand, G11R and A88V

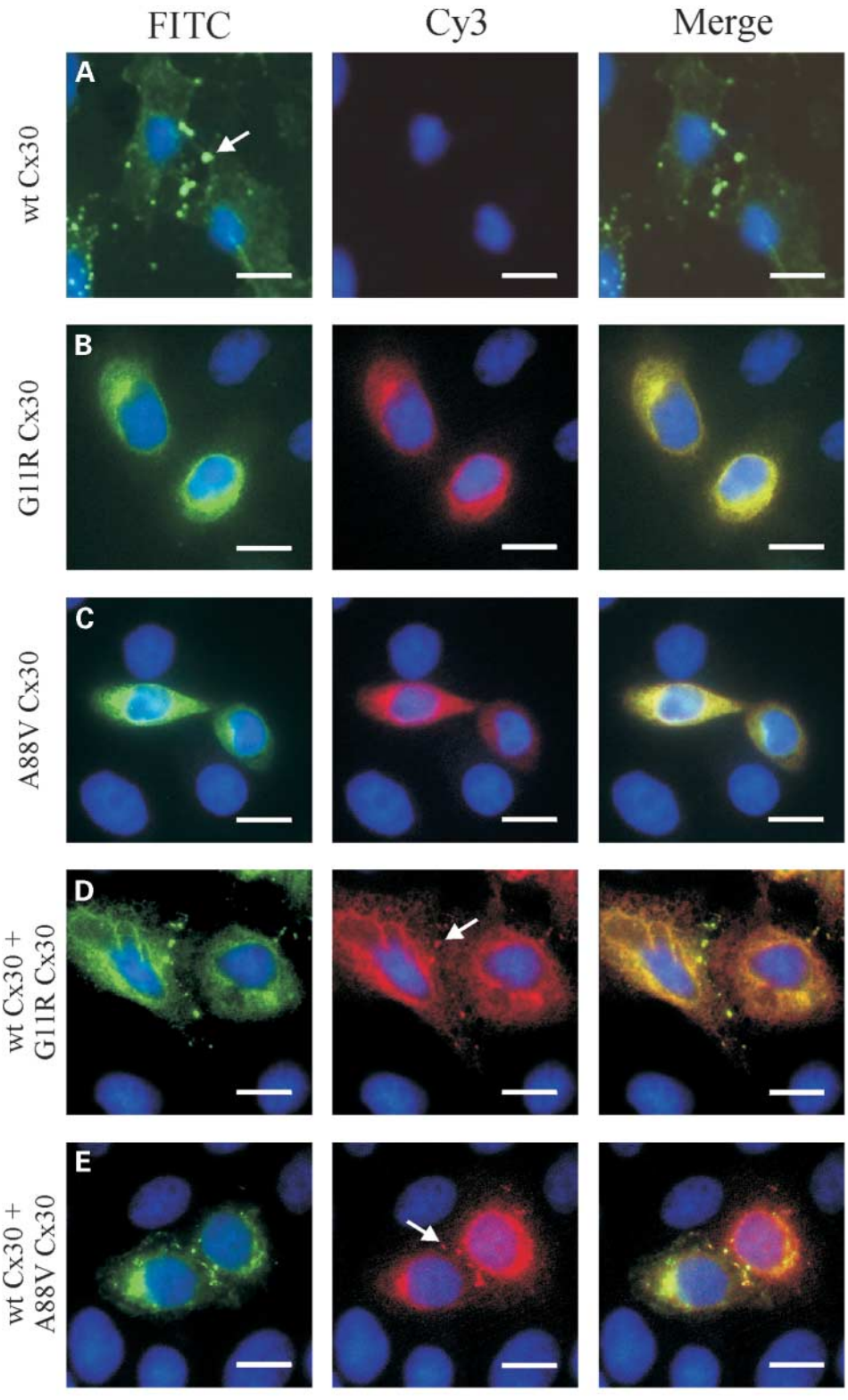

Figure 2. Wild-type and mutant forms of Cx30 co-localize in transfected HeLa cells. The wild-type form of the transfected protein lacked the V5 tag, which was present on the mutated forms. For this reason, wt Cx30 was only recognized by the anti-Cx30 antibody (green fluorescence), whereas G11R and A88V Cx30 were recognised by both the anti-Cx30 and the anti-V5 antibodies (green and red fluorescence). (**A**) Cells transfected with wt Cx30 show the protein (green fluorescence) at membrane interfaces (arrow). In contrast, cells transfected with either G11R Cx30 (**B**) or A88V Cx30 (**C**) exclusively show a cytoplasmic localization of the protein (green and red fluorescence). (**D** and **E**) When co-transfected with wt Cx30, the two mutated proteins (green and red fluorescence) were detected at the interface of cells (arrows). Scale bar 10 μm. Nuclei are stained with DAPI (blue fluorescence).

Cx30 were recognized by both the anti-Cx30 and the anti-V5 antibodies, and were detected as both green (FITC) and red fluorescence, thanks to a Cy3-labelled secondary anti-mouse antibody. Thus, a red labelling exclusively indicated a mutant Cx30. As previously reported (12), transfections with wt Cx30 led to large areas of staining at the membrane interface of HeLa cells (Fig. 2A). On the other hand, HeLa cells transfected with G11R or A88V Cx30 showed no obvious concentration of the proteins at the membrane (Fig. 2B and C). However, the cytoplasm of these cells was evenly stained in red, indicating an accumulation of the mutated connexins and making it difficult to exclude that limited amounts of the protein were targeted to the plasma membrane. After co-transfections of equal amounts of wild-type and mutated Cx30, we observed that the mutated connexins were co-expressed in both cytoplasm and membranes of the very same cells (Fig. 2D and E).

Mutant forms of Cx30 allow for dye coupling of HeLa cells as wt Cx30

To determine the permeability of the channels made of wild-type and mutated Cx30, we microinjected neurobiotin (NB, MW = 287 Da, 1 positive charge) and Lucifer yellow (LY, MW = 443 Da, 2 negative charges) in HeLa cells that had been transiently transfected either for one form of the connexin (wt Cx30, G11R Cx30 or A88V Cx30) or with a combination of the wild-type and a mutated form (wt plus G11R Cx30 or wt plus A88V Cx30). NB revealed coupling between HeLa cells, irrespective of the Cx30 form that had been transfected (Fig. 3 and Table 1). In most cases, the tracer diffused between three and 10 adjacent cells. No significant difference in the incidence of coupling was revealed between the five groups of cells which were compared. However, cells transfected for A88V Cx30 were often uncoupled and featured coupling limited to a median number of six cells labelled by NB after each injection ($n = 12$). In contrast, cells transfected for wt Cx30 were almost consistently coupled (the median number of cells labelled after each injection was 10, $n = 9$) (Table 1). Co-transfection of wt Cx30 with either G11R Cx30 or A88V Cx30 did not markedly alter this pattern (Fig. 3 and Table 1). The dependence of this coupling on junctional channels was established by assessing the lack of intercellular transfer of a 40 kDa molecular weight dextran, which was always retained within the individual cells that had been microinjected (Fig. 3F).

We also probed the transfected cells for exchange of LY. This tracer, which has a larger size and molecular weight than NB and a different electrical charge, may barely permeate Cx30 channels (13), presumably because its hydrated diameter closely corresponds to the pore of the gap junction channels (14). HeLa cells transfected with wt Cx30 showed a much reduced coupling incidence and extent when tested with LY than with NB. Thus, coupling was observed only between 2 and 4 cells after about 50% of the injections (Fig. 3 and Table 1). G11R Cx30 and A88V Cx30 also allowed for limited LY transfer after about 45% of the injections. Cells co-transfected for both the wt and a mutated form of Cx30

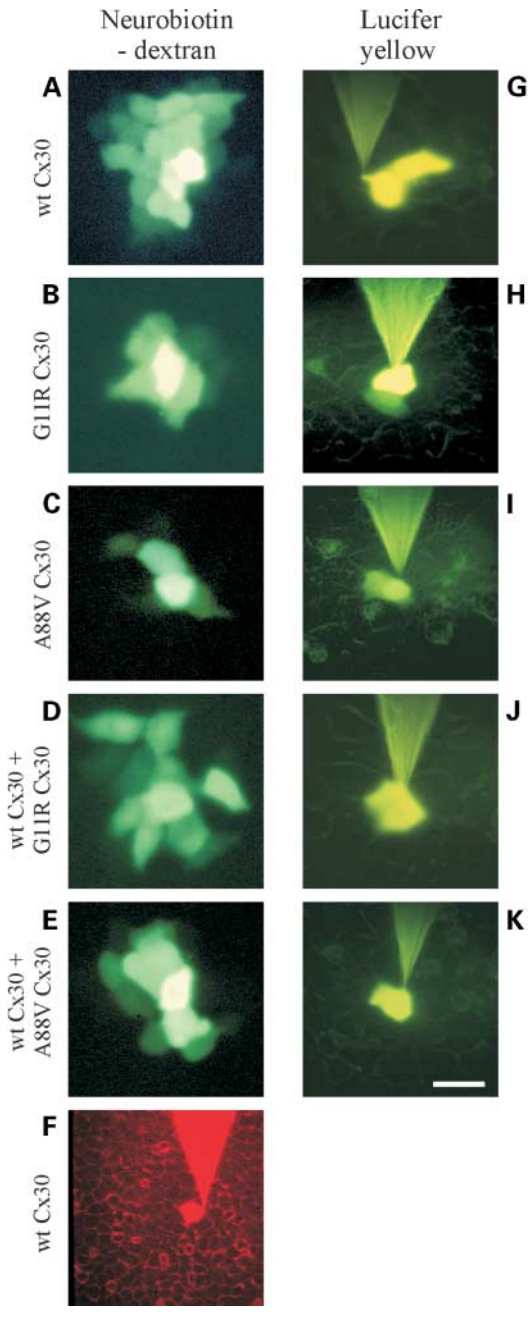

Figure 3. The wild-type and mutated forms of Cx30 permit a differential transfer of NB and LY between transfected HeLa cells. Left panel: injections of NB-dextran. (**A**) After a 5 min injection, most HeLa cells expressing the wild-type form of Cx30 exchanged NB with 5–10 of their neighbours. (**B** and **C**) A comparable dye coupling was observed between cells transfected with either G11R (B) or A88V Cx30 (C), or co-expressing the wild-type form of Cx30 and one of the mutations that are observed in Clouston syndrome (**D**: wt + G11R Cx30; **E**: wt + A88V Cx30). (**F**) No cell-to-cell transfer of a 40 kDa dextran was observed between the very same cells that had exchanged NB (the cell illustrated is the same shown in A). Right panel: injections of LY under conditions similar to those used for NB. (**G**) Most HeLa cells expressing the wild-type form of Cx30 exchanged LY with only 2–3 of their neighbours. (**H** and **I**) A comparable transfer was observed between cells transfected with either G11R (H) or A88V Cx30 (I). (**J** and **K**) LY transfer was not significantly altered between HeLa cells co-expressing wt Cx30 and either the G11R Cx30 (J) or the A88V Cx30 mutated form of the connexin (K). Scale bar 15 μm.

Table 1. The wt and mutated forms of Cx30 mediate a differential transfer of LY and NB between transfected HeLa cells

Transfected HeLa cells	No. cells injected	No. cells labelled by					
		Lucifer yellow			Neurobiotin		
	LY / NB	1[a]	2	≥3	1[a]	2	≥3
Wt Cx30	16/9	7	5	4	0	2	7
G11R Cx30	18/11	10	7	1	2	3	6
A88V Cx30	18/12	10	8	0	3	7	2
G11R Cx30 + wt Cx30	17/13	11	4	2	2	4	7
A88V Cx30 + wt Cx30	18/11	10	5	3	1	3	7

[a]Uncoupling.

did not behave differently than the cells transfected with only one form of the connexin (Fig. 3 and Table 1).

G11R and A88V Cx30 form functional intercellular channels in paired *Xenopus* oocytes

The ability of G11R and A88V Cx30 to form functional channels was tested using paired *Xenopus* oocytes, in which intercellular currents developed by the injected connexin RNAs can be analyzed (15). The translational competence of the *in vitro* transcribed RNAs was examined in a rabbit reticulocyte lysate in the presence of [^{35}S]methionine (Fig. 4A). Both wild-type and mutated RNAs directed the synthesis of a major polypeptide band that, as in other studies (16), migrated with an electrophoretic mobility that differed from that predicted for a molecular mass of 30 kDa (Fig. 4A, lanes 1–3). Oocyte pairs expressing either G11R or A88V Cx30 efficiently assembled homotypic channels that resulted in conductance levels comparable with those recorded with wt Cx30 (Fig. 4B). We noticed, however, that the A88V mutation exhibited a reduced propensity to form gap junction channels with respect to either wt or G11R ($P < 0.025$). Thus, homotypically paired oocytes injected with wt and G11R Cx30 received the same amount of RNA (either 1 or 4 ng/cell, depending on the experiment), whereas in the case of A88V Cx30 consistent and reliable measurements of junctional conductance were obtained only when higher RNA amounts (32–40 ng/cell) were injected. Both G11R and A88V Cx30 retained the ability to interact equally well with wt Cx30 in heterotypic configuration and yielded levels of junctional conductance that were not different from those of homotypic wt–wt pairs (data not shown).

Homotypic G11R and A88V channels exhibit distinct voltage gating properties

To test whether the channels made by the two mutated forms of Cx30 had altered electrical properties and gating behaviour, we examined their response to voltage gating. The junctional currents of homotypic channels made of wt Cx30 decayed over time for potentials >40 mV (Fig. 5A), in agreement with previous studies (17,18), and the rate of channel closure increased with V_j. Boltzmann plots of the normalized steady-state conductance values measured at the end of the imposed pulses showed a symmetrical response to voltage (Table 2). Oocyte pairs expressing G11R Cx30 channels displayed a similar voltage dependence (Fig. 5C), as reflected by comparing the values of transjunctional voltage (V_0) required to elicit a conductance midway between G_{jmax} and G_{jmin} (Table 2). In contrast, at the larger $V_j$values, the residual conductance (G_{jmin}) of G11R Cx30 homotypic channels was significantly increased ($P < 0.01$) with respect to that of wt Cx30 for both depolarizing and hyperpolarizing pulses (Fig. 5D and Table 2). The voltage gating behaviour of homotypic channels made of A88V Cx30 revealed a more pronounced sensitivity to voltage. Thus, junctional currents started to decay at potentials $> \pm 20$ mV (Fig. 5E), and, accordingly, the V_0 values were lower ($P < 0.01$), when compared with those of either wt or G11R Cx30 channels (Table 2).

G11R and A88V Cx30 form voltage-activated hemichannels

As mentioned in the Materials and Methods section, the injection of RNAs encoding G11R and A88V Cx30 was toxic for oocytes, unless the Ca^{2+} concentration of the culture medium was raised to 2.9 mM, suggesting the presence of functional hemichannels. To test for the presence of such hemichannels, we recorded whole cell currents of single *Xenopus* oocytes, in the presence of 2.9 mM Ca^{2+} and in response to depolarizing voltage steps. As expected, antisense controls (Fig. 6A) displayed no evidence of voltage-activated currents. Oocytes injected with RNA for wt Cx30 showed small currents at the more positive potentials (Fig. 6B), indicating the formation of some hemichannels, as previously reported (19). Under the same experimental conditions, large, voltage-activated outward currents were consistently induced when oocytes expressing G11R Cx30 were stepped to voltages > -20 mV (Fig. 6C). Similar results were obtained with A88V Cx30 (data not shown). Quantitation of the current–voltage relationship demonstrated that, at +60 mV, A88V Cx30 and G11R Cx30 featured voltage-activated currents of hemichannels that were increased 3- and 5-fold, respectively, over those measured in oocytes expressing wt Cx30 (Fig. 6D).

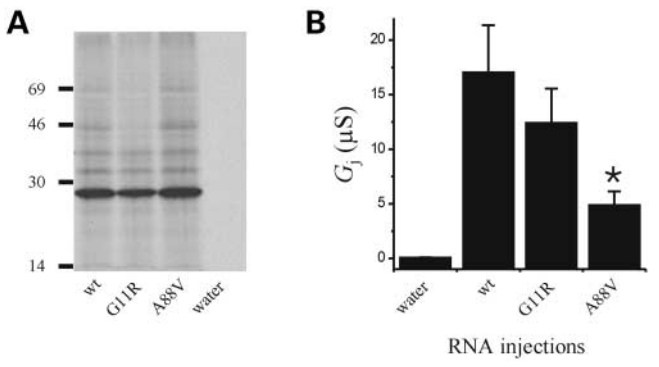

Figure 4. Wild-type, G11R and A88V Cx30 form functional intercellular channels in paired *Xenopus* oocytes. (**A**) Translational competence of synthetic RNAs encoding wt, G11R and A88V Cx30. Experimental conditions are indicated at the bottom of each lane. The molecular mass (in kDa) and migration of the protein standards are shown on the left edge of the gel. The *in vitro* translated products were separated on a 13% SDS–polyacrylamide gel, and detected by fluorography. Each RNA directed the synthesis of a major polypeptide product migrating with a similar electrophoretic mobility and an apparent molecular weight of ~28 kDa. (**B**) Oocytes were injected with either RNA (wt, G11R or A88V) or water and paired for 8–24 h before measuring junctional conductance (G_j) by dual voltage clamp. All cells were pretreated with antisense Cx38 oligonucleotides to deplete oocytes of the endogenously expressed connexin. Water-injected cells showed no detectable coupling under these conditions. G11R and A88V retained the ability to assemble homotypic junctional channels. Values are mean ± SEM of 34–39 oocyte pairs from at least five independent experiments. $^*P < 0.025$ versus either wt or G11R.

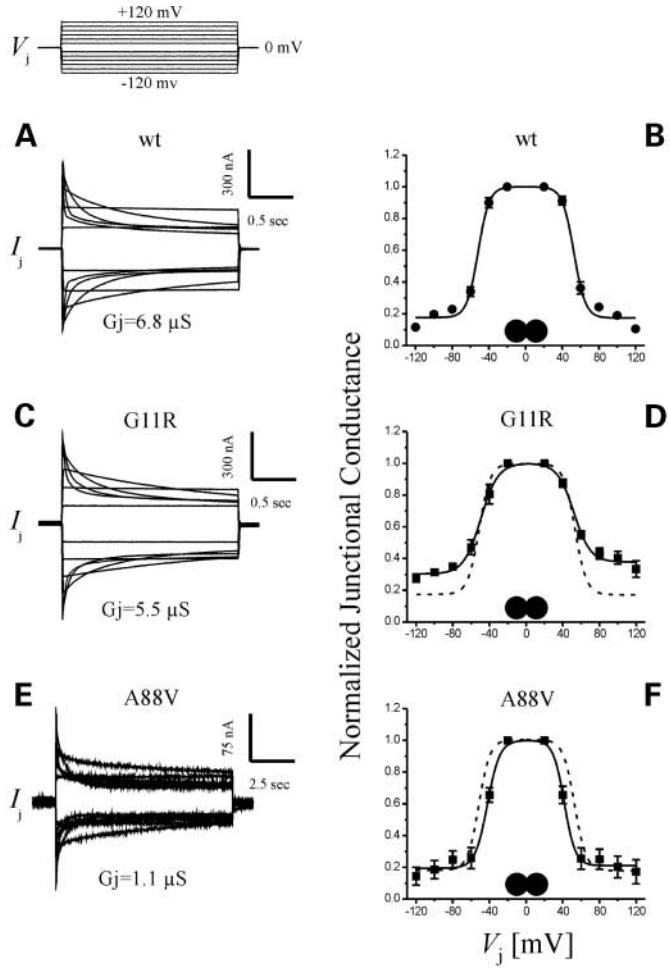

Figure 5. Homotypic channels composed of wt, G11R and A88V Cx30 are gated by transjunctional voltage. (**A**, **C**, **E**) Time-dependent decay of junctional currents developed by pairs of antisense-treated oocytes injected with RNAs coding for the specified constructs. The currents reflect voltage-induced closure of the cell-to-cell channels for transjunctional potentials (V_j) > ±40 mV whether those channels were made of wt (A), G11R (B) or A88V Cx30 (E). (**B**, **D**, **F**) Plots describe the relationship of V_j as a function of steady-state junctional conductance, normalised to the values obtained at ±20 mV. Solid lines represent the best fits to Boltzmann equations whose parameters are given in Table 2. For the sake of comparison, the dashed lines in (D) (G11R) and (F) (A88V) show the Boltzmann curve of Cx30 wt (B). Results represent mean ± SEM of 5–9 oocyte pairs from at least two independent experiments; in many cases, the error bars are contained within the plot symbols.

Mutant Cx30 causes ATP leakage in the extracellular medium and induces cell suffering

To assess the permeability of the hemichannels formed by G11R and A88V Cx30, we tested HeLa cells transfected for each of these mutated Cx30 for ATP leakage in the extracellular medium, and assessed whether this leakage was dependent on connexin hemichannels. Twenty-four hours after transfection, the relative luciferase activity indicating ATP release by transfected cells was expressed as percentage of that observed in the culture medium of mock-transfected control HeLa cells which were exposed to the transfection reagents without DNA. Mock-transfected cells, as well as cells that were transfected with a plasmid lacking the Cx30 insert (pcDNA^{TM}3.1/V5-His), and cells transfected with either wt Cx30 (wtCx30-pcDNA^{TM}3.1/V5-His) or the deafness-related T5M mutated Cx30 (T5MCx30-pcDNA^{TM}3.1/V5-His) showed similar levels of extracellular ATP (Fig. 7). In contrast, HeLa cells transfected with either G11R or A88V Cx30 (G11RCx30-pcDNA^{TM}3.1/V5-His and A88VCx30-pcDNA^{TM}3.1/V5-His), as well as cells doubly transfected with one of the mutated forms plus wt Cx30 showed levels of extracellular ATP that were 2–3 times greater ($P < 0.001$) than those observed in mock-transfected cells (Fig. 7). This increased ATP release was reduced to control levels ($P < 0.001$) following a 30 min exposure to α-glycyrrhetinic acid, a liquorice derivative that is widely used as an inhibitor of gap junction channels (Fig. 7). In order to make sure that such an increase in ATP release was not simply due to a higher proportion of dead cells that had been transfected with mutated Cx30, we have counted the relative number of viable cells [propidium iodide (PI)-negative] at 24 and 48 h following transfection. While no significant cell suffering was observed at 24 h following transfection, HeLa cells expressing the mutated forms of the protein presented a significantly greater number of PI-positive cells 48 h after transfection (Table 3).

DISCUSSION

Clouston syndrome or HED is a rare genodermatosis that mainly affects palmoplantar skin as well as ectodermic appendages (1). This disease is caused by mutations in the coding

Table 2. Parameters of homotypic channels composed of wt, G11R or A88V Cx30 in paired *Xenopus* oocytes

Channel	V_j	G_{jmax}	G_{jmin}	A	n	V_0
wt–wt ($n = 9$)	+	1	0.17 ± 0.01	0.19 ± 0.02	4.7 ± 0.6	53 ± 1
	−	1	0.17 ± 0.01	0.17 ± 0.02	4.3 ± 0.4	51 ± 2
G11R–G11R ($n = 6$)	+	1	0.36 ± 0.04*	0.14 ± 0.01	3.5 ± 0.3	52 ± 2
	−	1	0.31 ± 0.02*	0.15 ± 0.01	3.8 ± 0.3	48 ± 3
A88V–A88V ($n = 5$)	+	1	0.21 ± 0.01	0.19 ± 0.01	4.9 ± 0.1	41 ± 2*
	−	1	0.19 ± 0.05	0.16 ± 0.02	4.1 ± 0.4	42 ± 1*

To quantify the voltage gating characteristics of the different channels, the oocyte pairs presented in Fig. 5 were used to calculate the parameters derived from the best fits to the Boltzmann equation (see Materials and Methods). G_{jmin} is the minimum conductance value estimated from the Boltzmann fit, and V_0 is the voltage at which the half-maximal decrease of G_j is measured. The cooperativity constant (A), reflecting the voltage sensitivity of the channel, can also be expressed as the equivalent number (n) of electron charges moving through the transjunctional voltage field. The plus and minus signs for V_j refer to the polarity of the transjunctional potential. These parameters were derived from oocyte pairs whose G_j was 3.9± 0.6 μS ($n = 9$) for wt; 3.1± 0.8 μS ($n = 6$) for G11R and 2.9± 1.5 μS ($n = 5$) for A88V (mean± SEM).
*$P < 0.01$ versus the respective parameters of wt–wt channels.

region of the *GJB6* (Cx30) gene, but the mechanism whereby these mutations cause HED is unknown. In order to understand such mechanisms, we have studied the cellular transport of the G11R and A88V mutated forms of Cx30 as well as the functional properties of the channels formed by these mutated proteins in the presence and absence of wt Cx30.

By analogy to what has been reported in other genetic diseases associated to connexin mutations (20–22), Cx30 mutations may cause HED by altering the transport of the protein to the cell surface. In this study, we have first observed that the localization of Cx30 in palmoplantar skin of patients with HED is alike that of observed in unaffected individuals, with no detectable accumulation of the protein in the cytoplasm of keratinocytes. We have confirmed that, as previously described (12), both G11R and A88V are abundant in the cytoplasm of transfected HeLa cells. However, under conditions that recapitulate *in vitro* the heterozygous state of the affected individuals, i.e. after co-transfection with the native form of the protein, both G11R and A88V Cx30 were readily observed at membrane interfaces between cells. A sizeable fraction of the mutated forms of Cx30 which we studied were transported to the membranes of HeLa cells, both in the presence or in the absence of wt Cx30, as indicated by our dye injection experiments. Together, these results indicate that the two mutated forms of Cx30 that are associated with HED form cell-to-cell channels, but their accumulation at the plasma membrane is limited and may be masked, in immunostaining experiments, by their larger accumulation in the cytoplasm. It remains to be established whether this accumulation indicates some specific perturbation in the intracellular transport of the mutated proteins, as proposed in a previous report (12), or merely reflects a saturation of the transport machinery of the cells when high levels of the proteins are induced by transfection. It is noticeable that the presence of the T5M mutation (responsible for nonsyndromic autosomal dominant deafness at the DFNA3 locus) has been shown not to disturb the trafficking of the protein in transfected cells (12). This indicates that different mutations may have different effects on Cx30 trafficking.

In our experiments, dye coupling was more extensive when assessed with NB than when assessed with LY. Although the passage of the former tracer through Cx30 channels is in agreement with previous reports (23), that of LY was not anticipated since previous studies had indicated that human and mouse Cx30 may not allow for the transfer of this molecule (12,13). Several differences between our and these previous studies may explain this difference. First, our human Cx30 constructs contained a small, 29 amino acid V5-His tag, whereas previous studies tested the connexin tagged with the much larger, 273 amino acid green fluorescent protein (12), which could sterically hinder the entrance of LY into the hydrophilic centre of the junctional channels. Second, different levels of Cx30 expression between the HeLa cells stably transfected with mouse Cx30 (13) and our HeLa cells, which were transiently transfected with human Cx30, may also be relevant, since Cx30 forms low conductance channels (13,24), which favour the passage of small tracers (16), particularly when expressed in limited number. Thus, at variance with the deafness-related T5M mutated form of Cx30, which has been reported to form poorly permeant channels (12), both G11R and A88V Cx30 allowed for the easy passage of NB between adjacent HeLa cells. Co-expression of these proteins with wild-type Cx30 did not reveal an obvious dominant negative effect, inasmuch as dye injection showed frequent coupling of cells expressing a mixture of the two connexins. Quantitative evaluation revealed minor differences in the extent of dye transfer of the different cell groups that were compared, whereas junctional conductance was larger in cells connected by wild-type Cx30 than in cells expressing the G11R Cx30 form, or co-expressing either the latter protein or A88V Cx30 together with the native form of the connexin, suggesting subtle differences in the permeability of the resulting cell-to-cell channels. The electrophysiological analysis of paired *Xenopus* oocytes further revealed that the channels made by A88V Cx30 differed from those made by the other Cx30 forms in their voltage gating properties. Since the macroscopic junctional conductance (G_j) between two cells ($G_j = n \times P_0 \times \gamma_j$) is the product of the number of channels open at any given time (n) times the single channel open probability (P_0) times the single channel unitary conductance (γ_j), the lower values recorded in homotypic A88V pairs could be due to either one of two mechanisms, which are not mutually exclusive. First, the A88V mutation leads to a reduced inter-connexon affinity in

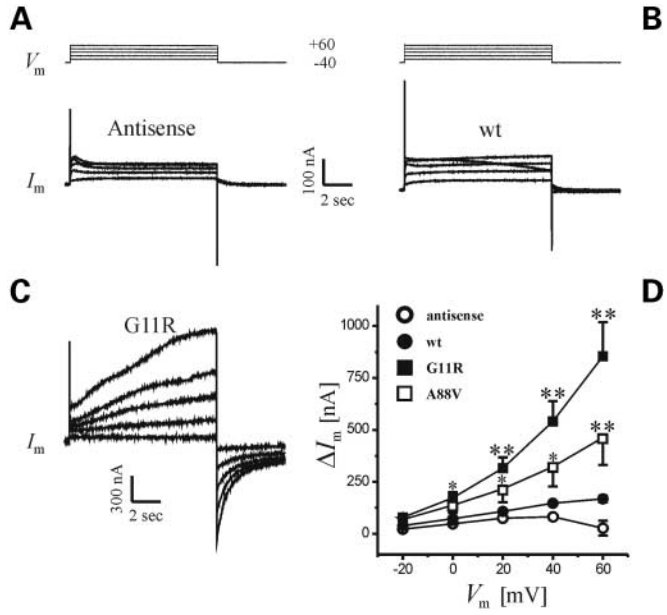

Figure 6. G11R and A88V mutations of Cx30 lead to the formation of functional hemichannels in single *Xenopus* oocytes. (**A**–**C**) Whole-cell membrane currents (I_m) were measured in single oocytes co-injected with the different Cx30 RNAs and an oligonucleotide antisense to *Xenopus* Cx38 (see Materials and Methods). Cells were initially clamped at a membrane potential (V_m) of −40 mV and depolarizing steps lasting 10 s were applied in 20 mV increments up to +60 mV (top traces in A and B). At positive membrane potentials, expression of both G11R (C) and A88V (data not shown) resulted in the activation of an outward current that was not seen in either the antisense-treated controls (A) or the cells injected with wt Cx30 RNA (B). (**D**) Current–voltage relationships were determined for oocytes injected with antisense oligonucleotides (open circles), wt Cx30 (solid circles), G11R Cx30 (solid squares), or A88V Cx30 (open squares) RNAs plus antisense. Peak current values above holding currents (ΔI_m) were calculated and plotted as a function of V_m. Starting at a V_m of 0 mV, the mean amplitude of hemichannel currents recorded in G11R- and A88V-injected cells was significantly different from that of control and wt Cx30 oocytes. $^*P < 0.01$ and $^{**}P < 0.005$. Results are shown as mean ± SEM from at least two independent experiments; in many cases, the error bars are contained within the plot symbols. Antisense ($n = 12$); wt ($n = 12$); G11R ($n = 14$) and A88V ($n = 4$).

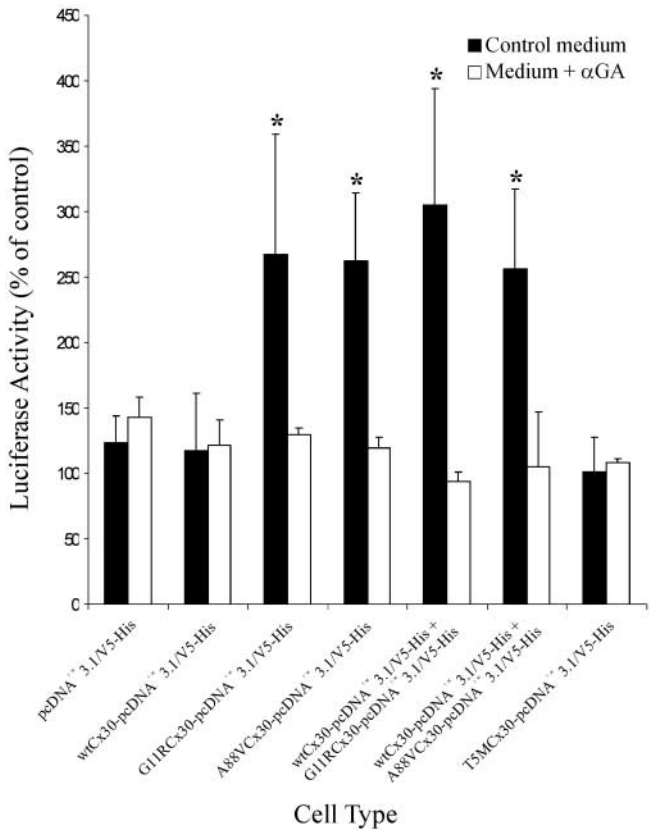

Figure 7. ATP release is increased after transfection of HeLa cells for either G11R or A88V Cx30. Extracellular ATP levels were evaluated by a luciferase activity assay and expressed relative to those measured in control cells that were exposed to the transfection reagent without plasmid DNA (100%). Cells transfected with wt Cx30 with T5M Cx30 as well as without a connexin cDNA (wtCx30-pcDNA™3.1/V5-His, T5MCx30-pcDNA™3.1/V5-His and pcDNA™3.1/V5-His, respectively) showed comparable extracellular ATP levels. Cells transfected with G11R or with A88V Cx30 (G11RCx30-pcDNA™3.1/V5-His and A88VCx30-pcDNA™3.1/V5-His, respectively) alone or co-transfected with one of these mutated constructs plus wt Cx30 showed a much larger ATP release, which was reduced to control levels after exposure to the uncoupling drug α-glycyrrhetinic acid. Values are mean ± SEM for $n > 6$ experiments. $^*P < 0.005$ significantly different from the mock-transfected control.

homotypic configuration, which results in a poor efficiency in channel formation, as previously shown for other mutant connexins (25,26). This possibility is supported by the observation that larger amounts of microinjected RNA (with respect to wt and G11R) are needed to obtain consistent levels of junctional conductance and by the finding that such a functional deficit was reversed by constructing heterotypic wt-A88V channels, which were as efficiently assembled as in the case of homotypic wt–wt pairs. Second, this amino acid substitution affects intrinsic channel properties that have an impact on the recorded levels of G_j, for example, favouring a closed state in the absence of transjunctional potential (27), as well as reducing the open time probability and/or unitary conductance, as demonstrated for other disease-causing connexin mutations (28,29). Further work at the single channel level is needed to distinguish between these possibilities. At any rate, the two Cx30 mutations we studied did not abolish intercellular coupling nor did they exert a major dominant negative effect on the junctional channels. Therefore, a decrease in cell-to-cell coupling cannot easily account for a pathogenetic role in the development of HED.

After the injection of single oocytes with either G11R or A88V Cx30 RNA, we unexpectedly observed a depigmentation of the cells, a loss of their membrane potential and, in most cases, their lysis, suggesting that, similarly to other wild-type and mutated connexins (30–32), the mutated species of Cx30 formed functional hemichannels in the non-junctional membrane. Although we did not examine in detail the long-term effect of the expression of Cx30 mutants on HeLa cells viability, we suspect, as previously described for other connexins (33,34), that these two mutations exerted adverse effects also in this expression system. Thus, we were unable to derive clones stably expressing any one of them and observed higher proportions of dead cells over time in the case of HED transfectants, as indicated by the increased number of PI-positive cells 48 h after transfection.

Table 3. Effect of Cx30 mutations on cell survival

Transfected HeLa cells		Control	Wt Cx30	G11R Cx30	A88V Cx30	Wt Cx30 + G11R Cx30	Wt Cx30 + A88V Cx30
24 h	% PI+ (SEM)	4.7 (3.9)	8.2 (4.7)	10.1 (6.0)	11.2 (2.8)	11.2 (0.6)	9.1 (4.3)
48 h	% PI+ (SEM)	2.6 (4.2)	18.2 (7.2)	37.0* (11.2)	42.3* (11.5)	23.8*,[a] (9.7)	30.1*,[b] (6.4)

Percentage of propidium iodide-positive (PI+) cells at 24 and 48 h following transfection; $n = 4$ experiments. Controls are HeLa cells transfected with a plasmid lacking the Cx30 insert.
*$P < 0.01$ versus the corresponding control.
[a]Not significantly different from cells transfected with G11R Cx30 alone.
[b]Not significantly different from cells transfected with A88V Cx30 alone.

It should be noted, however, that HeLa cells were cultured in the presence of 1.9 mM Ca^{2+}, a concentration well above that of the standard MB culture medium for oocytes, which could reduce hemichannel activity. The connexin nature of these hemichannels is supported by several lines of evidence. First, oocyte death could be prevented by raising the extracellular Ca^{2+} concentration that, as already reported for other connexin isoforms (35–39), strongly inhibits hemichannel activity. Second, oocytes expressing the mutated Cx30 exhibited large, voltage-activated outward currents that were barely detectable, even at the more positive depolarizing steps, in either oocytes injected with wt Cx30 RNA or control cells (all tested in high external Ca^{2+} conditions). Third, the presence of open hemichannels made of mutated Cx30 was consistent with the finding of a large ATP leakage from HeLa cells that had been transfected with either G11R or A88V Cx30, alone or together with wild-type Cx30, but not from cells that expressed wt Cx30 or the deafness-related T5M mutation of this protein. Finally, the ATP release in the extracellular medium could be prevented by incubating HeLa cells in the presence of the gap junction blocker α-glycyrrhetinic acid. We are aware that these liquorice derivatives are not entirely specific for gap junction blockade and that it remains possible that ATP release occurs via other types of α-glycyrrhetinic acid-sensitive channels, whose expression may have been induced in HeLa transfected for a mutated Cx30 and that we have not provided a definitive proof that hemichannels are the only source of ATP release. Since the number of viable cells expressing a mutated form of Cx30 was similar to that of HeLa transfected with wt Cx30 at 24 h after transfection, cell death cannot account for the increase in extracellular ATP levels. Moreover, ATP measurements were performed on cells that had been washed and incubated in the presence of fresh medium for only 15 min. However, on the basis of numerous observations obtained by different laboratories that have consistently correlated the finding of an α-glycyrrhetinic acid-sensitive ATP release to the presence of functional hemichannels (40), the simplest interpretation of our data is that the two mutated forms of Cx30 that are associated to HED not only form typical, cell-to-cell gap junction channels, but also hemichannels that show a propensity to open after insertion in the non-junctional membrane. It is possible, therefore, that the *in vivo* keratinocyte hyperproliferation observed in HED is due to an uncontrolled release, via open hemichannels, of ATP and other metabolites that may alter the paracrine signalling within the epidermis.

Connexins are best known for their role in the formation of channels between the cytoplasms of two adjacent cells, but more recent studies have highlighted the ability of some members of the connexin family to also form functional hemichannels (41). Thus, unpaired connexons have been shown to be activated under a variety of experimental conditions (40,42) and to play a role in the propagation of calcium waves through ATP release (43,44). Hemichannel properties are similar to those of paired connexons, and connexin-dependent ATP release has been shown to be regulated by extra- and intracellular calcium, at least *in vitro* (45,46). Abnormal ATP leakage from keratinocytes, via mutated Cx30 hemichannels, provides a conceivable molecular mechanism of HED. Indeed, it has been shown that, in both normal and pathological skin, extracellular ATP plays an important role in the regulation of keratinocyte differentiation and proliferation via the activation of specific purinergic receptors (47,48). This mechanism may also be relevant for other connexin-related skin diseases, inasmuch as mutations of Cx31, which are responsible for EKV (10), are also lethal for HeLa cells (47). Clearly, however, not all connexin mutations result in the formation of such hemichannels, as exemplified by our findings with the T5M mutation of Cx30. Thus, the mechanisms underlying the hearing loss phenotype associated to T5M Cx30 differ from that causing HED, which results, *in vitro*, in a toxic gain of function of the G11R and A88V mutations that remains to be verified *in vivo* in the epidermis of the HED patients. Another relevant point concerning the study of these connexin mutations is that Cx30 has been shown not only to interact with wt Cx26 but also with its skin-related D66H mutated form, both in the inner ear and in rodent skin (33,50). It is thus possible to imagine that G11R and A88V Cx30 retain the ability to form heterotypic channels with other connexins and that such interactions might, for example, improve their trafficking to the membrane and help to explain the absence of accumulation of mutated Cx30 in the cytoplasm of affected keratinocytes.

Our results have uncovered a plausible mechanism underlying the development of HED and open new pathways to be explored in the study of connexin pathology. Future studies should establish whether other connexins expressed in human skin (51,52), and notably those whose mutations have been associated to genodermatosis (10), are also able to form functional hemichannels and how they interact with one another. If so, the specific physiological and pathophysiological functions these hemichannels serve in epidermis will have to be clarified.

MATERIALS AND METHODS

Cx30 constructs

The entire coding sequence of the wild-type human *GJB6* gene was amplified by PCR from genomic DNA (using sense primer: 5′-GGATAAACCAGCGCAATG-3′; antisense primer: 5′-GCTTGGGAAACCTGTGTATTG-3′) and cloned into the pcDNA^{TM}3.1/V5-His vector (Invitrogen), under control of the CMV promoter (wtCx30-pcDNA^{TM}3.1/V5-His). The insert's open reading frame was cloned in phase with the V5-His coding sequence of the vector. Specified Cx30 mutations were obtained by site-directed mutagenesis (QuickChange Site Directed Mutagenesis Kit, Stratagene) using the following primers: for G11RCx30-pcDNA^{TM}3.1/V5-His (sense: 5′-CACTTTCATCAGGGGTGTCAACAAAC ACTCC-3′; antisense: 5′-GGAGTGTTTGTTGACACCCCTG ATGAAATGT-3′); for A88VCx30-pcDNA^{TM}3.1/V5-His (sense: 5′-CGTCTCCACCCCAGTGCTGCTGGTGGCC-3′; antisense: 5′-GGCCACCAGCAGCACTGGGGTGGAGACG-3′); for T 5MCx30-pcDNA^{TM}3.1/V5-His (sense: 5′-GGATTGGGGGA TGCTGCACACT TTCATCGG-3′; antisense: 5′-CCGAT GAAAGTGTGCAGCATCCCCCAATCC-3′). In order to reintroduce the original stop codon of Cx30, which had been removed for cloning into the expression vector and thus prevent the translation of the epitope tags, a fifth construct (wtCx30-pcDNA^{TM}3.1/stop) was obtained using the wtCx30-pcDNA^{TM}3.1/V5-His vector as the template, with the following mutagenic primers (sense: 5′-CACAGGTTT CCCAAGCTAGGGCAATTCTGC-3′; antisense: 5′-GCAG AATTGCCCTAGCTTGGGAAACCTGTG-3′). All constructs were verified for unwanted amino acid changes by automated sequencing.

Cell culture and transfection

HeLa cells were cultured in Dulbecco's modified Eagle's medium supplemented with 10% fetal calf serum, 1 U/ml penicillin and 1 μg/ml streptomycin. Cells were seeded 24 h before transfection at a density of 10^4 cells/cm^2. Transfection was carried out using the Effectene^{TM} (Qiagen) transfection reagent. Briefly, 100 000 cells were plated in 1.6 ml of medium and 1 μg plasmid DNA was added to the supplied buffer EC in a final volume of 50 μl, followed by 1.5 μl Enhancer and 5 μl Effectene^{TM} transfection reagent. Culture medium (600 μl) was then added to the mixture and the reagents were added to the cells. About 55–65% of the cells were positive for the transfected protein 24 h after transfection.

Antibodies and immunostaining

We used a rabbit polyclonal antibody against Cx30 purchased from Zymed. The antibody against the V5 epitope was purchased from Invitrogen. FITC-conjugated anti-rabbit IgG and Cy3-conjugated anti-mouse IgG secondary antibodies were purchased from Jackson Immunoresearch.

Paraffin-embedded samples of normal and pathological skin were prepared as described (53). Primary antibody treatment (1/200) was performed overnight at 4°C and revealed using the DAKO LSAB®2 System. Briefly, slides were submitted to 10 min incubations with biotin-linked antibodies and peroxidase-labelled streptavidin followed by a diaminobenzidine treatment and a final counterstaining using haematoxylin.

HeLa cells cultured on microscope cover slips were stained 24 h after transfection. Briefly, cells were rinsed twice in phosphate-buffered saline (PBS) and kept for 3 min in acetone at −20°C. After a 30 min wash in PBS supplemented with 2% bovine serum albumin (BSA), cells were incubated with both anti-Cx30 (1/200) and anti-V5 (1/500) antibodies diluted in PBS–2%BSA for 2 h at room temperature. Cells were rinsed in PBS and incubated with the FITC-conjugated anti-rabbit antibodies and the Cy3-conjugated anti-mouse antibodies for 1 h. After further washing, slides were mounted using the DAPI-containing Vectashield® mounting medium (Vector).

Microinjection and dye transfer

For assessment of junctional coupling, individual cells were microinjected by iontophoresis within 1-day-old cultures, with either 4% LY CH (Sigma Chemical Co.) or a mixture of 5% NB (Vector Laboratories) and 1% dextran–rhodamine (Molecular Probes), as described (14,54). In the case of NB, the cultures were fixed in a 4% solution of paraformaldehyde in 0.1 M phosphate buffer, rinsed in PBS supplemented with 0.25% Triton X-100 (PBS-T) for 30 min, and exposed for 60 min to a fluorescein-conjugated streptavidin (Jackson Immunoresearch Laboratories), diluted 1:300. In all cases, the percentage of microinjections that resulted in cell-to-cell transfer of each tracer, as well as the number of cells stained by a gap junction tracer (1 cell = no coupling) was determined on photographs taken immediately after each microinjection (54). Data were analyzed by the nonparametric chi square test, as provided by the Statistical Package for Social Sciences software (SPSS, Chicago).

Functional expression in *Xenopus* oocytes

The coding sequence of wt Cx30, G11R Cx30 and A88V Cx30 were subcloned into the pSP64T expression vector (55), and capped RNAs were produced using the mMessage mMachine kit (Ambion). Stage V–VI oocytes were prepared following previously described protocols (56). All cells were injected with a total volume of 40 nl of either an antisense oligonucleotide (3 ng/cell), to suppress the endogenous *Xenopus* Cx38, or a mixture of antisense (as above) plus the specified Cx30 RNA (0.5–40 ng/cell). In preliminary experiments, we noticed that the injection of both G11R and A88V Cx30 RNAs resulted in depigmentation, loss of membrane potential and cellular lysis of most oocytes. These findings suggested an abnormal opening of hemichannels in the nonjunctional membrane, as already reported for other connexins (30–32). Since currents of most connexins hemichannels can be drastically reduced by raising extracellular Ca^{2+} (35–39), all subsequent experiments were performed in MB medium containing 2.9 mM Ca^{2+}.

For biochemical analysis, aliquots (300 ng) of *in vitro* synthesized RNAs were translated in a rabbit reticulocyte lysate system (Promega Corporation), in the presence of [^{35}S]methionine (New England Nuclear) and analyzed as previously described (57).

The set-up, hardware and software used for electrophysiological measurements and data analysis were as previously described (58,59). To study the hemichannel activity of wt and mutated Cx30, nonjunctional current recordings were obtained from single oocytes 8–24 h after RNA injection, using a two-electrode voltage-clamp procedure. Cells were clamped at −40 mV, and whole cell currents recorded in response to depolarizing voltage steps (from −20 to +60 mV, in 20 mV increments) imposed for 10 s. Current outputs were sampled at 100 Hz, and the calculated peak values above holding currents (ΔI_m) were plotted against membrane potential. The formation of intercellular channels was assessed following previously described protocols (59). Data were analyzed using Origin 6.0 (Microcal Software) and fit to a Boltzmann relation as previously described (59). Results are shown as mean ± SEM. Statistical analysis was performed using the Student's unpaired *t*-test, with a significance threshold set at *P* values of 0.05 or less.

Extracellular ATP measurements and cell survival analysis

ATP release was measured 24 h after transfection. Cells were cultured and transfected in 35 mm plates, rinsed twice in PBS and incubated in 400 µl fresh medium for 15 min at 37°C. Then 90 µl supernatant was collected and added to 90 µl nucleotide releasing reagent of the Vialight™ HS kit (Biowhittaker). After 20 min, 20 µl ATP monitoring reagent was added to the mixture, and luciferase activity was measured for 10 s on a EG&G Berthold Microplate LB96V luminometer.

Connexin channels were blocked by incubating cells for 30 min in medium containing 50 µM α-glycyrrhetinic acid (Sigma) (60). An aliquot of 400 µl of this medium was used for the 15 min incubation preceding the measurement of ATP release. Results were expressed as a mean ± SEM percentage of the luciferase activity observed in mock-transfected (exposure to transfection reagent without DNA) control HeLa cells.

Viability of the transfected cells was assessed by staining with the membrane-impermeable dye propidium iodide (PI). Transfected cells were incubated for 24 and 48 h then rinsed and treated with 500 ng/µl PI (Clontech) for 5 min. Dead (PI-positive) and viable (PI-negative) cells were counted and data were expressed as a percentage of total cells scored. Statistical analysis was performed using a *t*-test for unpaired observations, with a *P* value <0.01 considered to be significant.

ACKNOWLEDGEMENTS

We thank G. Gruel and M. Martin for helpful discussions. Work of the Meda group was supported by grants from the Swiss National Foundation (3100-067788.02), the Juvenile Diabetes Research Foundation International (1-2001-622 and 5-2004-255), the European Union (QLRT-2001-01777) and the National Institute of Health (DK63443-01). The work of the Bruzzone group was supported by a grant from the Pasteur–Weizmann joint research programme. The work of the Waksman group was supported by grants from the Ministère de la Jeunesse, de l'Education et de la Recherche (France) and the Commissariat à l'Energie Atomique. G.M.E. is the recipient of a PhD Fellowship from the Ministère de la Jeunesse, de l'Education et de la Recherche (France).

REFERENCES

1. Ando, Y., Tanaka, T., Horiguchi, Y., Ikai, K. and Tomono, H. (1988) Hidrotic ectodermal dysplasia: a clinical and ultrastructural observation. *Dermatologica*, **176**, 205–211.
2. Fraser, F.C. and Der Kaloustian, V.M. (2001) A man, a syndrome, a gene: Clouston's hidrotic ectodermal dysplasia (HED). *Am. J. Med. Genet.*, **100**, 164–168.
3. Tan, E. and Tay, Y.K. (2000) What syndrome is this? Hidrotic ectodermal dysplasia (Clouston syndrome). *Pediatr. Dermatol.*, **17**, 65–67.
4. Kibar, Z., Dube, M.P., Powell, J., McCuaig, C., Hayflick, S.J., Zonana, J., Hovnanian, A., Radhakrishna, U., Antonarakis, S.E., Benohanian, A. *et al.* (2000) Clouston hidrotic ectodermal dysplasia (HED): genetic homogeneity, presence of a founder effect in the French Canadian population and fine genetic mapping. *Eur. J. Hum. Genet.*, **8**, 372–380.
5. Lamartine, J., Munhoz Essenfelder, G., Kibar, Z., Lanneluc, I., Callouet, E., Laoudj, D., Lemaitre, G., Hand, C., Hayflick, S.J., Zonana, J. *et al.* (2000) Mutations in GJB6 cause hidrotic ectodermal dysplasia. *Nat. Genet.*, **26**, 142–144.
6. Smith, F.J., Morley, S.M. and McLean, W.H. (2002) A novel connexin 30 mutation in Clouston syndrome. *J. Invest. Dermatol.*, **118**, 530–532.
7. Evans, W.H. and Martin, P.E. (2002) Gap junctions: structure and function (Review). *Mol. Membr. Biol.*, **19**, 121–136.
8. Sohl, G. and Willecke, K. (2003) An update on connexin genes and their nomenclature in mouse and man. *Cell Commun. Adhes.*, **10**, 173–180.
9. White, T.W. and Paul, D.L. (1999) Genetic diseases and gene knockouts reveal diverse connexin functions. *Annu. Rev. Physiol.*, **61**, 283–310.
10. Richard, G. (2003) Connexin gene pathology. *Clin. Exp. Dermatol.*, **28**, 397–409.
11. Di, W.L., Rugg, E.L., Leigh, I.M. and Kelsell, D.P. (2001) Multiple epidermal connexins are expressed in different keratinocyte subpopulations including connexin 31. *J. Invest. Dermatol.*, **117**, 958–964.
12. Common, J.E., Becker, D., Di, W.L., Leigh, I.M., O'Toole, E.A. and Kelsell, D.P. (2002) Functional studies of human skin disease- and deafness-associated connexin 30 mutations. *Biochem. Biophys. Res. Commun.*, **298**, 651–656.
13. Manthey, D., Banach, K., Desplantez, T., Lee, C.G., Kozak, C.A., Traub, O., Weingart, R. and Willecke, K. (2001) Intracellular domains of mouse connexin26 and -30 affect diffusional and electrical properties of gap junction channels. *J. Membr. Biol.*, **181**, 137–148.
14. Meda, P. (2001) Assaying the molecular permeability of connexin channels. *Methods Mol. Biol.*, **154**, 201–224.
15. Dahl, G., Miller, T., Paul, D., Voellmy, R. and Werner, R. (1987) Expression of functional cell-cell channels from cloned rat liver gap junction complementary DNA. *Science*, **236**, 1290–1293.
16. Green, C.R., Harfst, E., Gourdie, R.G. and Severs, N.J. (1988) Analysis of the rat liver gap junction protein: clarification of anomalies in its molecular size. *Proc. R. Soc. Lond. B Biol. Sci.*, **233**, 165–174.
17. Dahl, E., Manthey, D., Chen, Y., Schwarz, H.J., Chang, Y.S., Lalley, P.A., Nicholson, B.J. and Willecke, K. (1996) Molecular cloning and functional expression of mouse connexin-30, a gap junction gene highly expressed in adult brain and skin. *J. Biol. Chem.*, **271**, 17903–17910.
18. Beltramello, M., Bicego, M., Piazza, V., Ciubotaru, C.D., Mammano, F. and D'Andrea, P. (2003) Permeability and gating properties of human connexins 26 and 30 expressed in HeLa cells. *Biochem. Biophys. Res. Commun.*, **305**, 1024–1033.
19. Valiunas, V. and Weingart, R. (2000) Electrical properties of gap junction hemichannels identified in transfected HeLa cells. *Pflugers Arch.*, **440**, 366–379.
20. VanSlyke, J.K., Deschenes, S.M. and Musil, L.S. (2000) Intracellular transport, assembly, and degradation of wild-type and disease-linked mutant gap junction proteins. *Mol. Biol. Cell.*, **11**, 1933–1946.
21. Gottfried, I., Landau, M., Glaser, F., Di, W.L., Ophir, J., Mevorah, B., Ben-Tal, N., Kelsell, D.P. and Avraham, K.B. (2002) A mutation in GJB3 is associated with recessive erythrokeratodermia variabilis (EKV) and leads to defective trafficking of the connexin 31 protein. *Hum. Mol. Genet.*, **11**, 1311–1316.

22. D'Andrea, P., Veronesi, V., Bicego, M., Melchionda, S., Zelante, L., Di Iorio, E., Bruzzone, R. and Gasparini, P. (2002) Hearing loss: frequency and functional studies of the most common connexin26 alleles. *Biochem. Biophys. Res. Commun.*, **296**, 685–691.
23. Elfgang, C., Eckert, R., Lichtenberg-Frate, H., Butterweck, A., Traub, O., Klein, R.A., Hulser, D.F. and Willecke, K. (1995) Specific permeability and selective formation of gap junction channels in connexin-transfected HeLa cells. *J. Cell Biol.*, **129**, 805–817.
24. Harris, A.L. (2001) Emerging issues of connexin channels: biophysics fills the gap. *Q. Rev. Biophys.*, **34**, 325–472.
25. Bruzzone, R., White, T.W. and Paul, D.L. (1994) Expression of chimeric connexins reveals new properties of the formation and gating behavior of gap junction channels. *J. Cell Sci.*, **107**, 955–967.
26. Oh, S., Rubin, J.B., Bennett, M.V., Verselis, V.K. and Bargiello, T.A. (1999) Molecular determinants of electrical rectification of single channel conductance in gap junctions formed by connexins 26 and 32. *J. Gen. Physiol.*, **114**, 339–364.
27. Suchyna, T.M., Xu, L.X., Gao, F., Fourtner, C.R. and Nicholson, B.J. (1993) Identification of a proline residue as a transduction element involved in voltage gating of gap junctions. *Nature*, **365**, 847–849.
28. Oh, S., Ri, Y., Bennett, M.V., Trexler, E.B., Verselis, V.K. and Bargiello, T.A. (1997) Changes in permeability caused by connexin 32 mutations underlie X-linked Charcot-Marie-Tooth disease. *Neuron*, **19**, 927–938.
29. Abrams, C.K., Freidin, M.M., Verselis, V.K., Bennett, M.V. and Bargiello, T.A. (2001) Functional alterations in gap junction channels formed by mutant forms of connexin 32: evidence for loss of function as a pathogenic mechanism in the X-linked form of Charcot–Marie–Tooth disease. *Brain Res.*, **900**, 9–25.
30. Paul, D.L., Ebihara, L., Takemoto, L.J., Swenson, K.I. and Goodenough, D.A. (1991) Connexin46, a novel lens gap junction protein, induces voltage-gated currents in nonjunctional plasma membrane of *Xenopus* oocytes. *J. Cell Biol.*, **115**, 1077–1089.
31. Abrams, C.K., Bennett, M.V., Verselis, V.K. and Bargiello, T.A. (2002) Voltage opens unopposed gap junction hemichannels formed by a connexin 32 mutant associated with X-linked Charcot–Marie–Tooth disease. *Proc. Natl Acad. Sci. USA*, **99**, 3980–3984.
32. Gomez-Hernandez, J.M., de Miguel, M., Larrosa, B., Gonzalez, D. and Barrio, L.C. (2003) Molecular basis of calcium regulation in connexin-32 hemichannels. *Proc. Natl Acad. Sci. USA*, **100**, 16030–16035.
33. Bakirtzis, G., Choudhry, R., Aasen, T., Shore, L., Brown, K., Bryson, S., Forrow, S., Tetley, L., Finbow, M., Greenhalgh, D. *et al.* (2003) Targeted epidermal expression of mutant connexin 26 (D66H) mimics true Vohwinkel syndrome and provides a model for the pathogenesis of dominant connexin disorders. *Hum. Mol. Genet.*, **12**, 1737–1744.
34. Di, W.L., Monypenny, J., Common, J.E., Kennedy, C.T., Holland, K.A., Leigh, I.M., Rugg, E.L., Zicha, D. and Kelsell, D.P. (2002) Defective trafficking and cell death is characteristic of skin disease-associated connexin 31 mutations. *Hum. Mol. Genet.*, **11**, 2005–2014.
35. Ebihara, L. and Steiner, E. (1993) Properties of a nonjunctional current expressed from a rat connexin46 cDNA in *Xenopus* oocytes. *J. Gen. Physiol.*, **102**, 59–74.
36. Li, H., Liu, T.F., Lazrak, A., Peracchia, C., Goldberg, G.S., Lampe, P.D. and Johnson, R.G. (1996) Properties and regulation of gap junctional hemichannels in the plasma membranes of cultured cells. *J. Cell Biol.*, **134**, 1019–1030.
37. Pfahnl, A. and Dahl, G. (1999) Gating of cx46 gap junction hemichannels by calcium and voltage. *Pflugers Arch.*, **437**, 345–353.
38. Bruzzone, S., Guida, L., Zocchi, E., Franco, L. and De Flora, A. (2001) Connexin 43 hemi channels mediate Ca^2+-regulated transmembrane NAD+ fluxes in intact cells. *FASEB J.*, **15**, 10–12.
39. Zoidl, G., Bruzzone, R., Weickert, S., Kremer, M., Zoidl, C., Mitropoulou, G., Srinivas, M., Spray, D.C. and Dermietzel, R. (2004) Molecular cloning and functional expression of zfCx52.6: a novel connexin with hemichannel-forming properties expressed in horizontal cells of the zebrafish retina. *J. Biol. Chem.*, **279**, 2913–2921.
40. Bennett, M.V., Contreras, J.E., Bukauskas, F.F. and Saez, J.C. (2003) New roles for astrocytes: gap junction hemichannels have something to communicate. *Trends Neurosci.*, **26**, 610–617.
41. Goodenough, D.A. and Paul, D.L. (2003) Beyond the gap: functions of unpaired connexon channels. *Nat. Rev. Mol. Cell Biol.*, **4**, 285–294.
42. Tran Van Nhieu, G., Clair, C., Bruzzone, R., Mesnil, M., Sansonetti, P. and Combettes, L. (2003) Connexin-dependent inter-cellular communication increases invasion and dissemination of Shigella in epithelial cells. *Nat. Cell Biol.*, **5**, 720–726.
43. Stout, C.E., Costantin, J.L., Naus, C.C. and Charles, A.C. (2002) Intercellular calcium signaling in astrocytes via ATP release through connexin hemichannels. *J. Biol. Chem.*, **277**, 10482–10488.
44. Leybaert, L., Braet, K., Vandamme, W., Cabooter, L., Martin, P.E. and Evans, W.H. (2003) Connexin channels, connexin mimetic peptides and ATP release. *Cell Commun. Adhes.*, **10**, 251–257.
45. Braet, K., Aspeslagh, S., Vandamme, W., Willecke, K., Martin, P.E., Evans, W.H. and Leybaert, L. (2003) Pharmacological sensitivity of ATP release triggered by photoliberation of inositol-1,4,5-trisphosphate and zero extracellular calcium in brain endothelial cells. *J. Cell. Physiol.*, **197**, 205–213.
46. Contreras, J.E., Saez, J.C., Bukauskas, F.F. and Bennett, M.V. (2003) Gating and regulation of connexin 43 (Cx43) hemichannels. *Proc. Natl Acad. Sci. USA*, **100**, 11388–11393.
47. Greig, A.V., Linge, C., Terenghi, G., McGrouther, D.A. and Burnstock, G. (2003) Purinergic receptors are part of a functional signaling system for proliferation and differentiation of human epidermal keratinocytes. *J. Invest. Dermatol.*, **120**, 1007–1015.
48. Denda, M., Inoue, K., Fuziwara, S. and Denda, S. (2002) P2X purinergic receptor antagonist accelerates skin barrier repair and prevents epidermal hyperplasia induced by skin barrier disruption. *J. Invest. Dermatol.*, **119**, 1034–1040.
49. Diestel, S., Richard, G., Doring, B. and Traub, O. (2002) Expression of a connexin31 mutation causing erythrokeratodermia variabilis is lethal for HeLa cells. *Biochem. Biophys. Res. Commun.*, **296**, 721–728.
50. Marziano, N.K., Casalotti, S.O., Portelli, A.E., Becker, D.L. and Forge, A. (2003) Mutations in the gene for connexin 26 (*GJB2*) that cause hearing loss have a dominant negative effect on connexin 30. *Hum. Mol. Genet.*, **12**, 805–812.
51. Salomon, D., Masgrau, E., Vischer, S., Ullrich, S., Dupont, E., Sappino, P., Saurat, J.H. and Meda, P. (1994) Topography of mammalian connexins in human skin. *J. Invest. Dermatol.*, **103**, 240–247.
52. Wiszniewski, L., Limat, A., Saurat, J.H., Meda, P. and Salomon, D. (2000) Differential expression of connexins during stratification of human keratinocytes. *J. Invest. Dermatol.*, **115**, 278–285.
53. Sivan, V., Vozenin-Brotons, M.C., Tricaud, Y., Lefaix, J.L., Cosset, J.M., Dubray, B. and Martin, M.T. (2002) Altered proliferation and differentiation of human epidermis in cases of skin fibrosis after radiotherapy. *Int. J. Radiat. Oncol. Biol. Phys.*, **53**, 385–393.
54. Charollais, A., Gjinovci, A., Huarte, J., Bauquis, J., Nadal, A., Martin, F., Andreu, E., Sanchez-Andres, J.V., Calabrese, A., Bosco, D. *et al.* (2000) Junctional communication of pancreatic beta cells contributes to the control of insulin secretion and glucose tolerance. *J. Clin. Invest.*, **106**, 235–243.
55. Krieg, P.A. and Melton, D.A. (1984) Functional messenger RNAs are produced by SP6 *in vitro* transcription of cloned cDNAs. *Nucl. Acids Res.*, **12**, 7057–7070.
56. Mitropoulou, G. and Bruzzone, R. (2003) Modulation of perch connexin35 hemi-channels by cyclic AMP requires a protein kinase A phosphorylation site. *J. Neurosci. Res.*, **72**, 147–157.
57. Bruzzone, R., Haefliger, J.A., Gimlich, R.L. and Paul, D.L. (1993) Connexin40, a component of gap junctions in vascular endothelium, is restricted in its ability to interact with other connexins. *Mol. Biol. Cell*, **4**, 7–20.
58. White, T.W., Deans, M.R., O'Brien, J., Al-Ubaidi, M.R., Goodenough, D.A., Ripps, H. and Bruzzone, R. (1999) Functional characteristics of skate connexin35, a member of the gamma subfamily of connexins expressed in the vertebrate retina. *Eur. J. Neurosci.*, **11**, 1883–1890.
59. White, T.W., Srinivas, M., Ripps, H., Trovato-Salinaro, A., Condorelli, D.F. and Bruzzone, R. (2002) Virtual cloning, functional expression, and gating analysis of human connexin31.9. *Am. J. Physiol. Cell Physiol.*, **283**, C960–970.
60. Duval, N., Gomes, D., Calaora, V., Calabrese, A., Meda, P. and Bruzzone, R. (2002) Cell coupling and Cx43 expression in embryonic mouse neural progenitor cells. *J. Cell Sci.*, **115**, 3241–3251.